

Supplementary Information

A Family of Simple Benzene 1,3,5-Tricarboxamide (BTA) Aromatic Carboxylic Acid Hydrogels

Richard C. T. Howe,^a Adam P. Smalley,^a Alexander P. M. Guttenplan,^a Matthew W. R. Doggett,^a Mark D. Eddleston,^a Jin Chong Tan,^b and Gareth O. Lloyd^{*a}

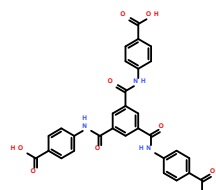
^a Department of Chemistry, University of Cambridge, Lensfield Road, Cambridge, United Kingdom, CB2 1EW.
Fax: (+) 44 1223 336362; Tel: (+) 44 1223 763989; E-mail: gol20@cam.ac.uk

^b Department of Engineering Science, University of Oxford, Parks Road, Oxford, United Kingdom, OX1 3PJ.

Synthesis

1,3,5-benzenetricarbonyl trichloride (3.98 g, 15.0 mmol) was added to a solution of amino aromatic carboxylic acid (45.1 mmol) and triethylamine (12.7 ml, 94.6 mmol) in 80ml tetrahydrofuran (THF). The mixture was stirred at room temperature for 16 hours under nitrogen. Water (300ml) was added, the mixture stirred vigorously for two hours. The white solid precipitate was filtered, followed by washing on the filter paper consecutively with acetone (25 ml), water (200 ml) and methanol (50 ml). This clean product was dried at 100 °C.

Compound 1



White solid (7.32 g, 86 % yield) and analysis matches that reported within the literature.

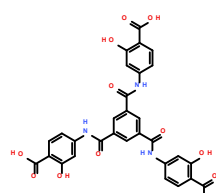
¹H NMR: (d₆-DMSO, J/Hz, δ/ppm): 12.70 (broad s, 3H, -CO₂H); 10.93 (s, 3H, -CONH-); 8.74 (s, 3H, Ar-H); 8.51 (d J=6.3, 6H, Ar-H); 7.80 (d J=6.3, 6H, Ar-H)

Elemental Analysis: calculated for (C₃₀H₂₁N₃O₉·3H₂O): C 58.0; H 4.4; N 6.8. Found: C 58.3; H 4.1; N 6.8.

MS: ES⁻ m/z = 566.1 [50%] M⁻.

IR (cm⁻¹): 3326, 3201, 3078, 2670, 2551, 1681, 1599, 1529, 1408, 1317, 1244, 1175, 1118, 1014, 956, 852, 768, 721, 690.

Compound 2



White-yellow solid (6.87 g, 74 % yield).

^1H NMR: (d_6 -DMSO, J/Hz, δ /ppm): 11.4 (broad s, 3H, -COOH), 10.82 (s, 3H, -CONH-), 8.68 (s, 3H, Ar-H), 7.79 (d, 3H, Ar-H), 7.55 (d, 3H, Ar-H), 7.35 (dd, 3H, Ar-H), 3.9 (very broad, 3H, -OH)

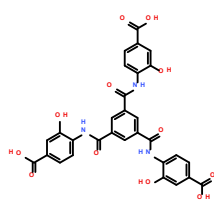
^{13}C NMR (d_6 -DMSO, δ /ppm): 172, 165, 162, 145, 135, 131, 131, 111, 109, 107.

Elemental Analysis: calculated for ($\text{C}_{30}\text{H}_{21}\text{N}_3\text{O}_{12} \cdot 2\text{H}_2\text{O}$): C 55.3; H 3.9; N 6.5. Found: C 55.1; H 3.7; N 6.1.

MS: ES $^-$ m/z = 614.1 [100%] M $^-$.

IR (cm^{-1}): 713, 775, 1157, 1237, 1539, 1597, 1643, 1658, 1665, 1678, 1687, 1733, 1772, 3074, 3734.

Compound 3



White-yellow solid (6.49 g, 70 % yield).

^1H NMR: (d_6 -DMSO, J/Hz, δ /ppm): 12.85 (broad s, 3H, -COOH), 10.35 (s, 3H, -CONH-), 9.90 (s, 3H, Ar-H), 8.68 (s, 3H, Ar-H), 7.94 (d, 3H, Ar-H), 7.50 (d, 3H, Ar-H), 3.4 (br, 3H, -OH)

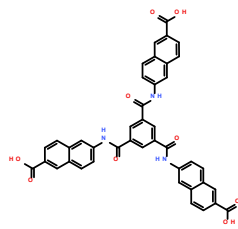
^{13}C NMR (d_6 -DMSO, δ /ppm): 167.2, 164.6, 162.5, 148.9, 135.0, 130.1, 127.8, 123.5, 120.7, 116.3.

Elemental Analysis: calculated for ($\text{C}_{30}\text{H}_{21}\text{N}_3\text{O}_{12} \cdot 6\text{H}_2\text{O}$): C 49.8; H 4.6; N 5.8. Found: C 49.7; H 4.6; N 5.5.

MS: ES $^-$ m/z = 614.1 [100%] M $^-$.

IR (cm^{-1}): 720, 763, 1212, 1281, 1424, 1529, 1558, 1576, 1605, 1642, 1658, 1678, 1691, 3207.

Compound 4



Off-white solid (9.90 g, 92 % yield).

^1H NMR: (d_6 -DMSO, J/Hz, δ /ppm): 13.02 (s, 3H, -CO₂H), 11.00 (s, 3H, -CONH-), 8.88 (s, 3H, Ar-H), 8.61 (d, J=14.2, 6H, Ar-H), 8.17 (t, J=8.1, 3H, Ar-H), 8.01 (m, 9H, Ar-H).

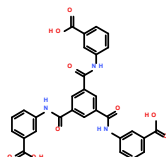
^{13}C NMR (d_6 -DMSO, δ /ppm): 167.6, 165.0, 162.4, 138.8, 135.7, 135.5, 130.4, 130.1, 129.2, 127.9, 127.1, 125.9, 121.5, 116.3.

Elemental Analysis: calculated for ($\text{C}_{42}\text{H}_{27}\text{N}_3\text{O}_9 \cdot \text{DMF} \cdot \text{H}_2\text{O}$): 66.8; H 4.5; N 6.9. Found: C 66.3; H 4.5; N 6.9.

MS: ES $^-$ m/z = 716.2 [11%] M $^-$; 566.1 [100%] ($\text{C}_{31}\text{H}_{20}\text{N}_2\text{O}_8 \cdot \text{H}_2\text{O}$) $^-$; 547.1 [54%] $\text{C}_{31}\text{H}_{19}\text{N}_2\text{O}_8^-$

IR (cm^{-1}): 695, 807, 1194, 1233, 1341, 1390, 1457, 1480, 1547, 1576, 1627, 1678, 1691, 2056, 3067.

Compound 5



White solid (7.98 g, 91 % yield).

^1H NMR: ($\text{d}_6\text{-DMSO}$, J/Hz , δ/ppm): 12.9 (broad s, 3H, $-\text{CO}_2\text{H}$); 10.78 (s, 3H, $-\text{CONH-}$); 8.77 (s, 3H, Ar-H); 8.44 (s, 3H, Ar-H); 8.10 (d $J=9$, 3H, Ar-H); 7.72 (d $J=9$, 3H, Ar-H); 7.52 (t $J=9$, 3H, Ar-H).

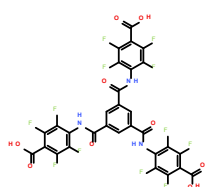
^{13}C NMR ($\text{d}_6\text{-DMSO}$, δ/ppm): 167.3, 164.8, 139.3, 135.4, 131.5, 130.2, 129.2, 125.0, 124.6, 121.3.

Elemental Analysis: calculated for ($\text{C}_{30}\text{H}_{21}\text{N}_3\text{O}_9 \cdot \text{H}_2\text{O}$): C 61.5, H 4.0, N 7.2. Found: C 61.0; H 4.1; N 7.1.

MS: ES^- m/z = 566.1 [100%] M^- .

IR (cm^{-1}): 646, 749, 1168, 1189, 1246, 1307, 1484, 1535, 1596, 1643, 1657, 1709, 3070, 3314.

Compound 6



White solid (4.00 g, 34 % yield).

^1H NMR: ($\text{d}_6\text{-DMSO}$, δ/ppm): 13.41 (s, 3H, $-\text{CO}_2\text{H}$); 8.61 (s, 3H, $-\text{CONH-}$); 6.64 (s, 3H, Ar-H).

^{13}C NMR ($\text{d}_6\text{-DMSO}$, δ/ppm): 165.9; 161.5; 147.0; 144.6; 136.4; 134.0; 133.7; 132.0.

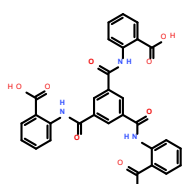
^{19}F NMR ($\text{d}_6\text{-DMSO}$, δ/ppm): 142.2 (m, ^{12}F)

Elemental Analysis: calculated for ($\text{C}_{30}\text{H}_{9}\text{F}_{12}\text{N}_3\text{O}_9 \cdot \text{H}_2\text{O}$): C 45.0; H 1.4; N 5.2. Found: C 44.8; H 1.3; N 5.0.

MS: ES^- m/z = 782.01 [10%] M^- ; 591.01 [100%] $\text{C}_{23}\text{H}_7\text{F}_8\text{N}_2\text{O}_8^-$; 400.01 [80%] $\text{C}_{16}\text{H}_6\text{F}_4\text{NO}_7^-$.

IR (cm^{-1}): 639, 726, 869, 949, 1051, 1175, 1316, 1407, 1502, 1541, 1609, 1642, 1717, 1788, 3211, 3380, 3494, 3600, 3730.

Compound 7



White solid (7.49 g, 88 % yield).

¹H NMR: (d₆-DMSO, J/Hz, δ/ppm): 12.47 (s, 3H, -CONH-), 8.80 (s, 3H, Ar-H), 8.65 (d, 3H, J=8.4 Hz, Ar-H), 8.02 (d, 3H, J=8 Hz, Ar-H), 7.65 (t, 3H, J=8 Hz, Ar-H), 7.21 (t, 3H, J=7.6 Hz, Ar-H). Carboxylic acid not visible.

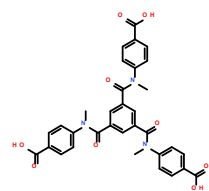
¹³C NMR (d₆-DMSO, δ/ppm): 170.29, 162.99, 140.77, 135.86, 134.43, 131.31, 128.90, 123.47, 120.20, 117.10.

Elemental Analysis: calculated for (C₃₀H₂₁N₃O₉·3H₂O): C 58.0; H 4.4; N 6.8. Found: C 57.5; H 4.3; N 6.5.

MS: ES⁻ m/z = 566.1 [100%] M⁻.

IR (cm⁻¹): 695, 715, 744, 956, 1150, 1244, 1301, 1450, 1529, 1590, 1665, 3483.

Compound 8



White solid (5.30 g, 58 % yield).

¹H NMR: (d₆-DMSO, J/Hz, δ/ppm): 13.0 (broad s, 3H, -COOH), 7.88 (d, J=8, 6H, Ar-H), 6.96 (s, 3H, Ar-H), 6.74 (d, 6H, J=8, Ar-H), 3.24 (s, 9H, N-CH₃).

¹³C NMR (d₆-DMSO, δ/ppm): 167.63, 166.53, 147.84, 135.76, 130.24, 129.15, 128.79, 126.86, 37.17.

Elemental Analysis: calculated for (C₃₃H₂₇N₃O₉·H₂O): C 63.2; H 4.7; N 6.7. Found: C 63.3; H 4.4; N 6.7.

MS: ES⁻ m/z = 608.2 [100%] M⁻.

IR (cm⁻¹): 695, 715, 744, 956, 1150, 1244, 1301, 1450, 1529, 1590, 1665, 3483.

Gelator Na salts.

Compounds **1 – 5** (5 mmoles) were dissolved in water (25 ml) by the addition of NaOH (16 mmoles) in water (10 ml). The sodium salts of the trianionic gelators was precipitated by the addition of 200 ml of isopropanol. The precipitate was filtered and dried over-night at 45°C. Gelator Na salts were used as is, once dried.

Gelation utilising glucono-δ-lactone.

Na salts of the gelators were dissolved in neutral distilled water. Glucono-δ-lactone was added at one equivalent per carboxylic acid group. Samples were left stationary and were found to set over several hours.

ClogP and pK_a evaluation.

ClogP values were determined for the neutral compound and for the trianionic compound utilising the software ChemBioDraw (similar values were determined using other software). pK_a calculated values were determined using the SPARC v4.6. Experimental apparent pK_a values were determined using the method described by Adam et al.^{ref} An example of the data for compound **2** obtained is shown below.

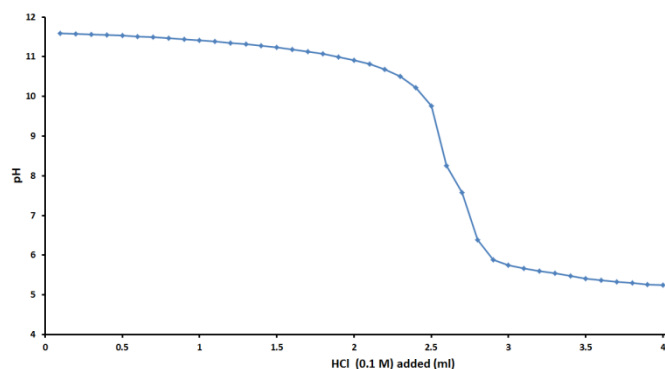


Figure S1. Titration of HCl in vigorously stirred solution of compound **2**. Data utilised to determine experimental apparent pK_a .

Powder X-Ray Diffraction (PXRD)

PXRD patterns were collected at room temperature using a Philips X'Pert Diffractometer operating at 40 kV and 40 mA with Cu K α radiation at a wavelength of 1.542 Å. Scans were run for 9 minutes. Gels were spread gently on a piece of filter paper in order to remove the excess solvent before application to a flat bracket. Crystals were dried thoroughly under vacuum filtration and ground to a powder. Patterns were viewed and analysed using the X'Pert HighScore Plus software. Powder patterns of crystal structures were generated from the Mercury 3.0 software.

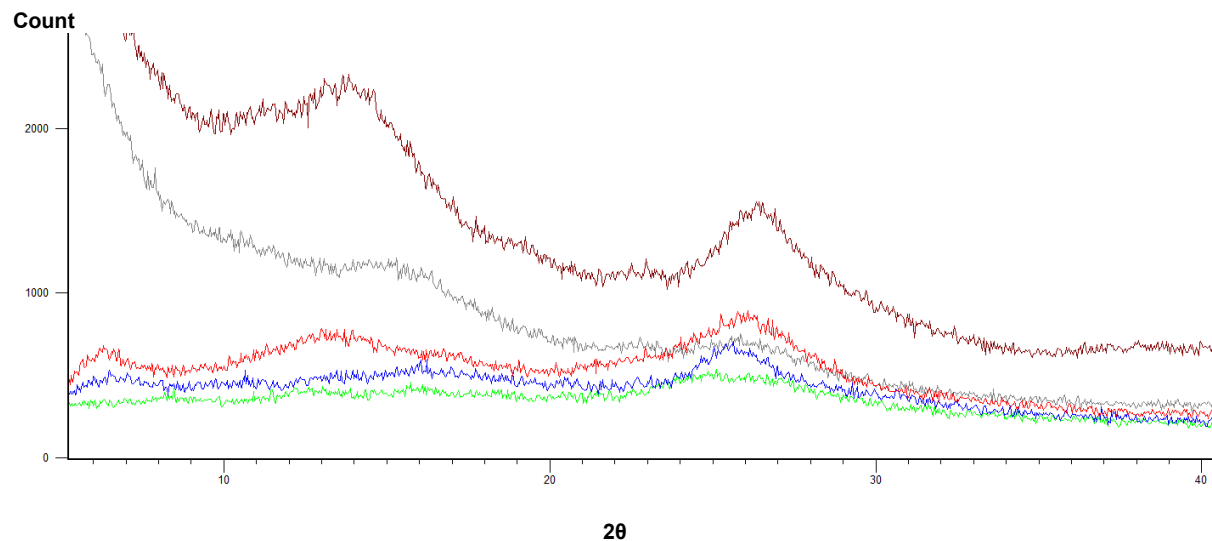


Figure S2. PXRD patterns of dried hydrogels of compounds **1** (blue), **2** (brown), **3** (grey), **4** (red) and **5** (green)) showing the characteristic d spacings at approximately 3.4 Å (26.5° 2θ).

Transmission Electron Microscopy (TEM)

A sample of the gel was wiped onto the TEM sample support grid using a pipette then placed into the TEM. A Philips CM30 instrument at an operating voltage of 300 kV was used. Images and diffraction patterns were collected on photographic film, which was subsequently scanned to produce digital images.

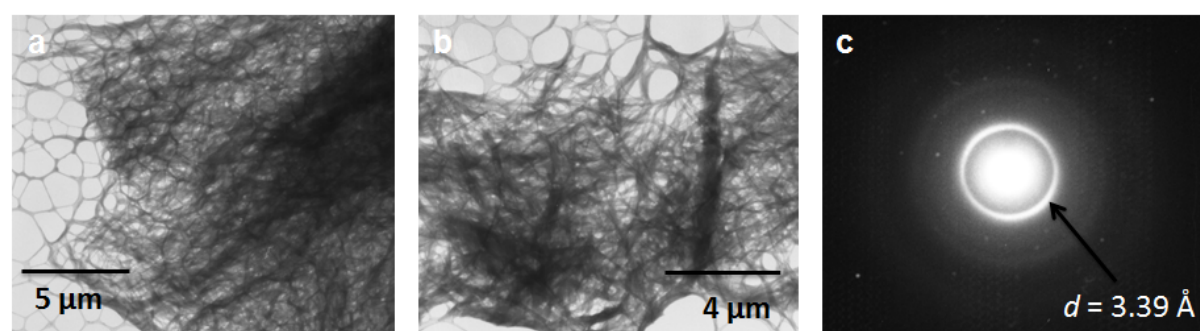


Figure S3. TEM images showing the fibrous nature of the 1 % by weight hydrogels formed with compound **1**.

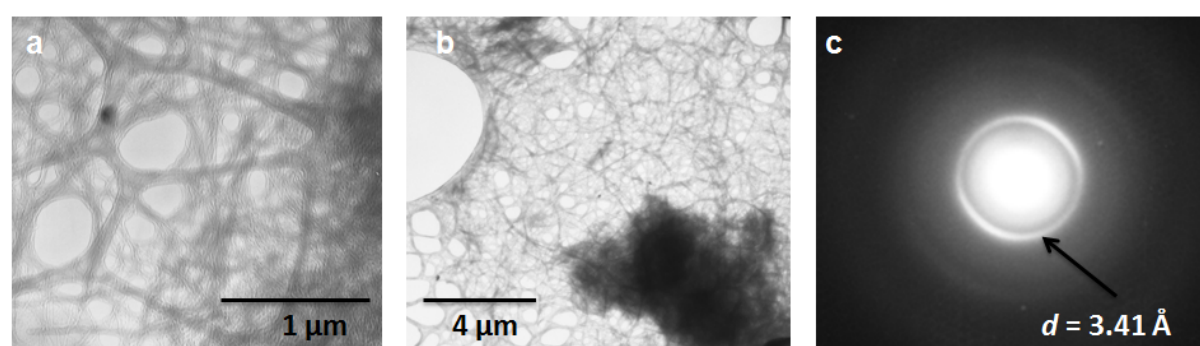


Figure S4. TEM images showing the fibrous nature of the 1 % by weight hydrogels formed with compound **2**.

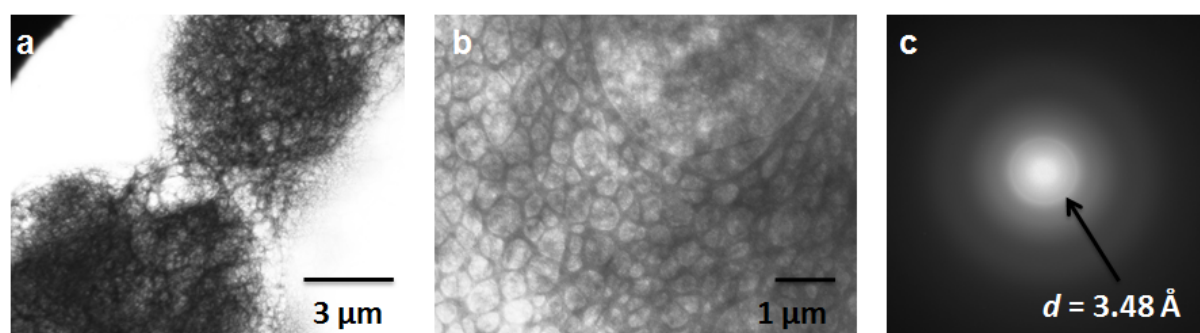


Figure S5. TEM images showing the fibrous nature of the 1 % by weight hydrogels formed with compound **3**.

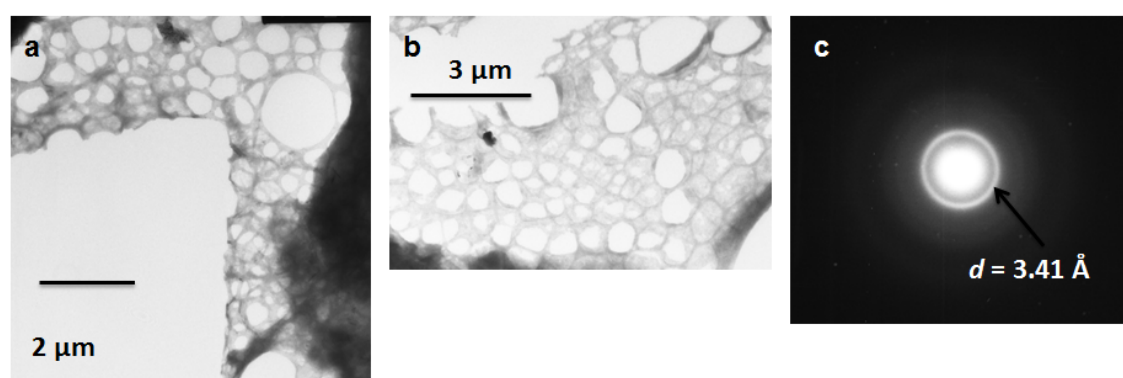


Figure S6. TEM images showing the fibrous nature of the 1 % by weight hydrogels formed with compound **4**.

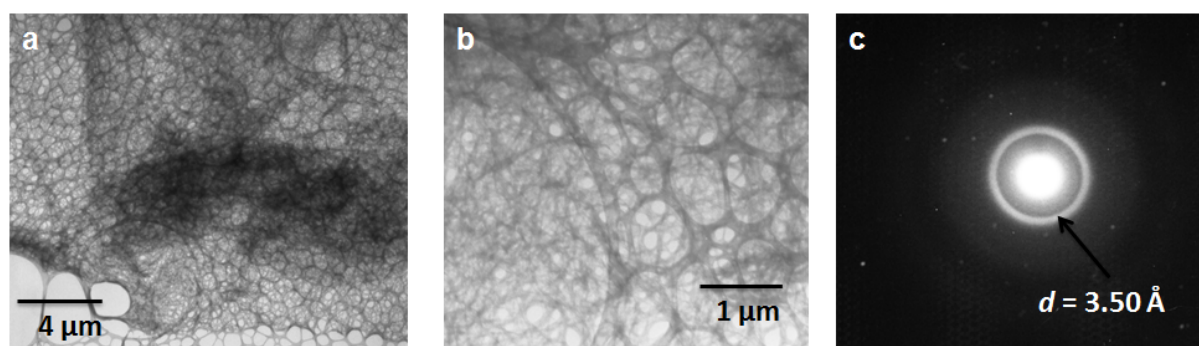


Figure S7. TEM images showing the fibrous nature of the 1 % by weight hydrogels formed with compound 5.

Cryo-Scanning Electron Microscopy

Samples of the gels were studied using a Philips XL30 SEM. The gels, again at 1% weight by volume were plunged into liquid nitrogen, and then transferred to the cryo-stage of the microscope. Once in place, the temperature was slowly raised to -95°C, allowing the water to be etched away and exposing the gel structure. This allows the gels to be imaged while avoiding damage from the high vacuum or from drying of the samples. Compounds 1, 2 and 5 were analysed and representative images are shown below.

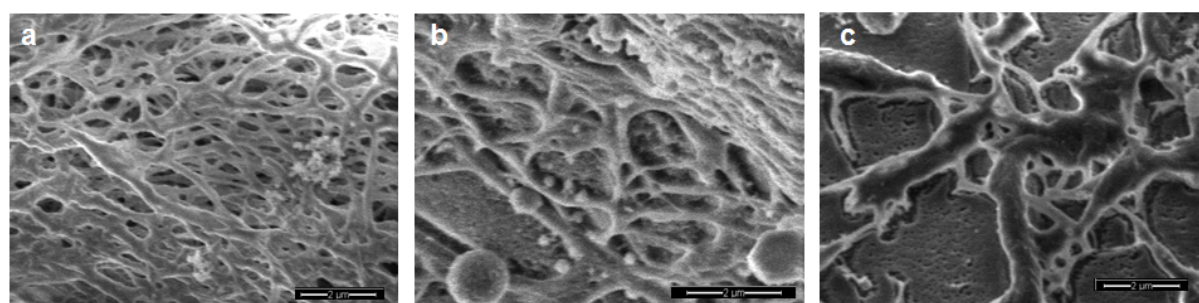


Figure S8. Cryo-SEM images showing the fibrous nature of the 1 % by weight hydrogels formed with compounds a) 1, b) 2 and c) 5.

Rheology

Rheological characterisation was performed on a DHR-3 produced by TA Instruments. An aluminium concentric cylinder (dimensions: $r_{\text{Bob}} = 13.99 \text{ mm}$, $r_{\text{cup}} = 15.00 \text{ mm}$, bob length = 42.08 mm) was used in all calculations at an operating gap of 100 μm. For all gels, 10 ml of the solution (gelator and glucono-δ-lactone) was added to the cup at the operating gap via syringe so that the gel could form around the bob. Data was collected and analysed using the TRIOS software produced by TA Instruments. Data presented here is for gels at 1 % by weight.

All time oscillations were initiated immediately after the insertion of the solutions. For all samples this was performed at 20 °C for 15h, a torque of 100 μNm and a frequency of 10 Hz. Data was taken every 30 s for a sampling time of 3 s.

Frequency oscillations were performed after the time oscillation at 20 °C. The torque was maintained at 100 μNm and 10 data points per decade were taken between 0.0159 and 100 Hz.

Amplitude oscillations of each gel were taken after the frequency oscillations experiments to measure the critical stress before breaking. The temperature was held at 20 °C. A frequency of 1 Hz was used and 10 data points per decade were taken between a torque of 10 and 200000 μNm.

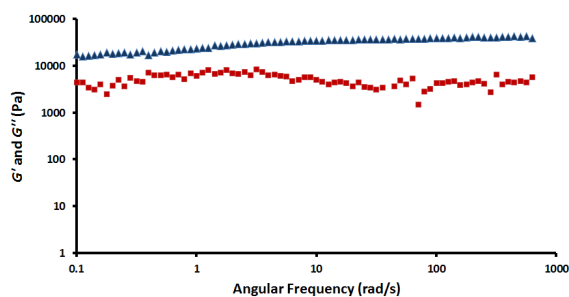


Figure S9. Frequency sweep rheometry of compound 1. The angular frequency (rad/s), storage modulus G' (Pa) and loss modulus G'' (Pa) are shown as log scale.

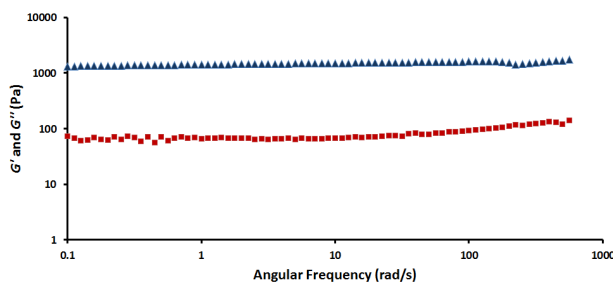


Figure S10. Frequency sweep rheometry of compound 2. The angular frequency (rad/s), storage modulus G' (Pa) and loss modulus G'' (Pa) are shown as log scale.

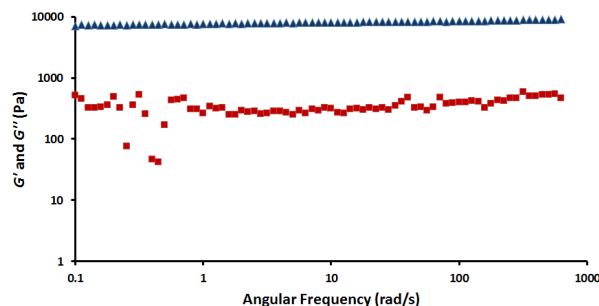


Figure S11. Frequency sweep rheometry of compound 3. The angular frequency (rad/s), storage modulus G' (Pa) and loss modulus G'' (Pa) are shown as log scale.

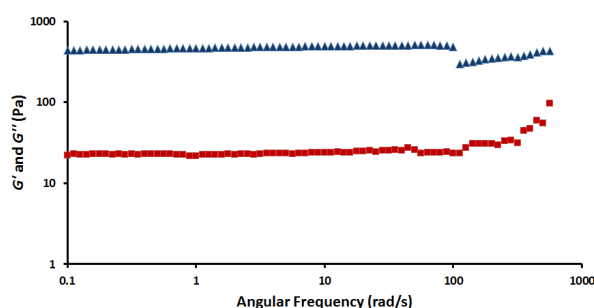


Figure S12. Frequency sweep rheometry of compound 4. The angular frequency (rad/s), storage modulus G' (Pa) and loss modulus G'' (Pa) are shown as log scale.

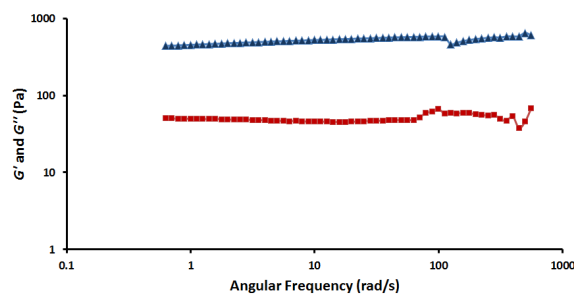


Figure S13. Frequency sweep rheometry of compound **5**. The angular frequency (rad/s), storage modulus G' (Pa) and loss modulus G'' (Pa) are shown as log scale.

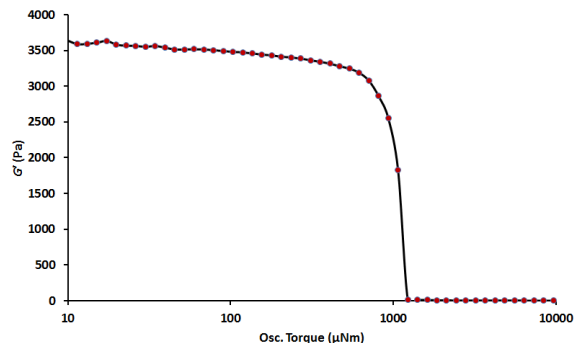


Figure S14. Osc. torque sweep rheometry of compound **1**. Osc. Torque (μNm) shown as log scale.

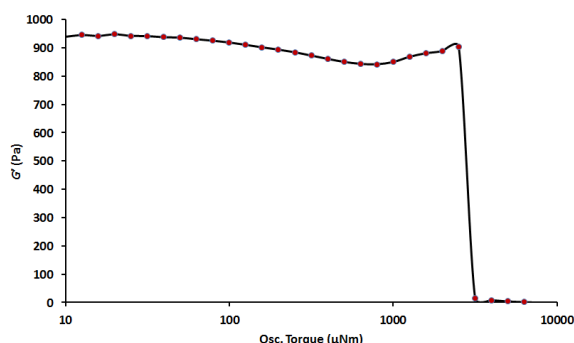


Figure S15. Osc. torque sweep rheometry of compound **2**. Osc. Torque (μNm) shown as log scale.

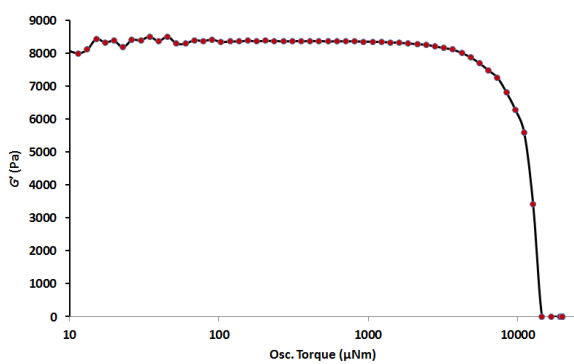


Figure S16. Osc. torque sweep rheometry of compound **3**. Osc. Torque (μNm) shown as log scale.

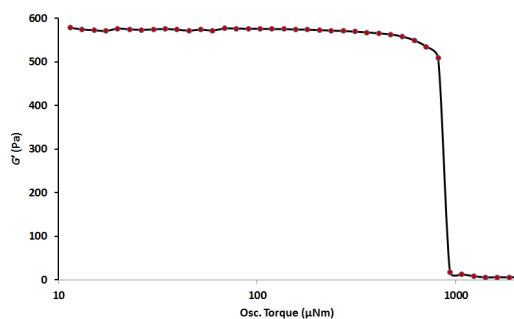


Figure S17. Osc. torque sweep rheometry of compound **4**. Osc. Torque (μNm) shown as log scale.

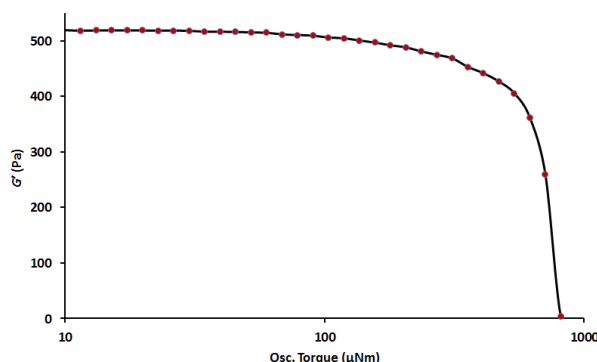


Figure S18. Osc. torque sweep rheometry of compound **5**. Osc. Torque (μNm) shown as log scale.

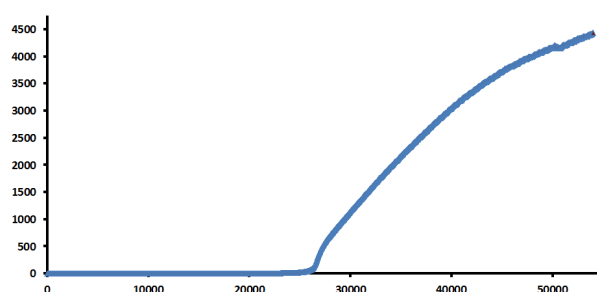


Figure S19. Time sweep rheometry of compound **1**. Storage modulus G' (Pa) (y axis) plotted against time (sec).

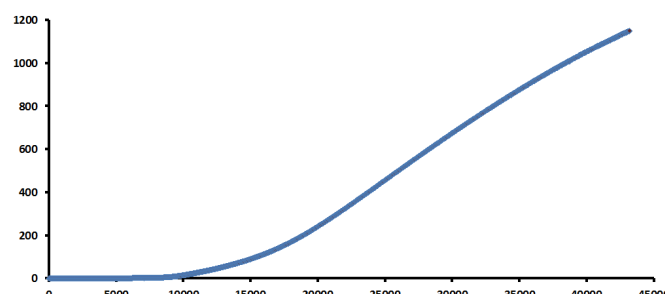


Figure S20. Time sweep rheometry of compound **2**. Storage modulus G' (Pa) (y axis) plotted against time (sec).

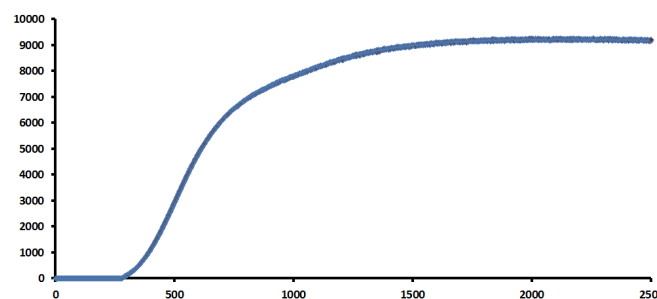


Figure S21. Time sweep rheometry of compound 3. Osc. Storage modulus G' (Pa) (y axis) plotted against time (sec).

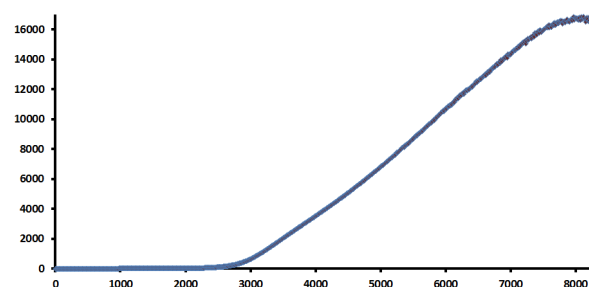


Figure S22. Time sweep rheometry of compound 4. Storage modulus G' (Pa) (y axis) plotted against time (sec), which is shown as log scale.

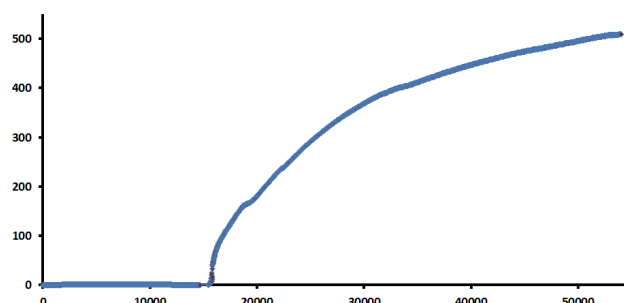


Figure S23. Time sweep rheometry of compound 5. Storage modulus G' (Pa) (y axis) plotted against time (sec).

X-ray Structure of compound 1

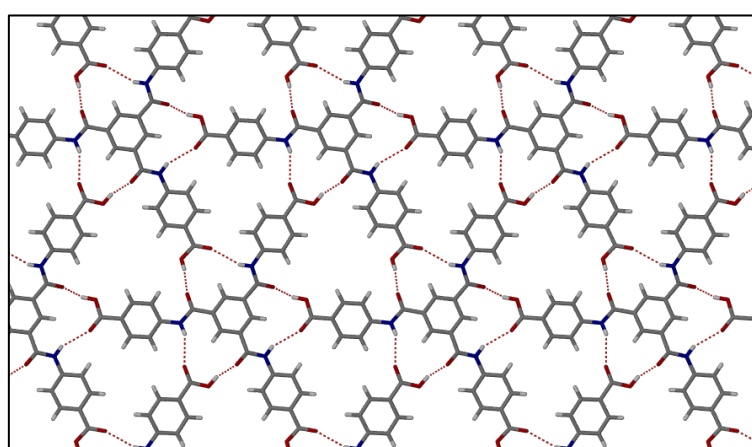


Figure S24. Crystal packing of compound 1 showing the hydrogen bonding between the amide and carboxylic acid groups to give a sheet structure, where the sheets mainly interacting through $\pi - \pi$ interactions.